

Article

Batch Syngas Fermentation by *Clostridium carboxidivorans* for Production of Acids and Alcohols

Fabiana Lanzillo ¹, Giacomo Ruggiero ¹, Francesca Raganati ^{1,*}, Maria Elena Russo ² and Antonio Marzocchella ¹

¹ Department of Chemical, Materials and Production Engineering—University of Naples Federico II, P.le V. Tecchio 80, 80125 Napoli, Italy; fabiana.lanzillo@unina.it (F.L.); giacomo.ruggiero@unina.it (G.R.); marzocch@unina.it (A.M.)

² Institute for Research on Combustion—National Research Council (CNR), P.le V. Tecchio 80, 80125 Napoli, Italy; m.russo@irc.cnr.it

* Correspondence: francesca.raganati@unina.it

Received: 29 June 2020; Accepted: 26 August 2020; Published: 1 September 2020



Abstract: Syngas (CO, CO₂, and H₂) has attracted special attention due to the double benefit of syngas fermentation for carbon sequestration (pollution reduction), while generating energy. Syngas can be either produced by gasification of biomasses or as a by-product of industrial processes. Only few microorganisms, mainly clostridia, were identified as capable of using syngas as a substrate to produce medium chain acids, or alcohols (such as butyric acid, butanol, hexanoic acid, and hexanol). Since CO plays a critical role in the availability of reducing equivalents and carbon conversion, this work assessed the effects of constant CO partial pressure (P_{CO}), ranging from 0.5 to 2.5 atm, on cell growth, acid production, and solvent production, using *Clostridium carboxidivorans*. Moreover, this work focused on the effect of the liquid to gas volume ratio (V_L/V_G) on fermentation performances; in particular, two V_L/V_G were considered (0.28 and 0.92). The main results included—(a) P_{CO} affected the growth kinetics of the microorganism; indeed, *C. carboxidivorans* growth rate was characterized by CO inhibition within the investigated range of CO concentration, and the optimal P_{CO} was 1.1 atm (corresponding to a dissolved CO concentration of about 25 mg/L) for both V_L/V_G used; (b) growth differences were observed when the gas-to-liquid volume ratio changed; mass transport phenomena did not control the CO uptake for V_L/V_G = 0.28; on the contrary, the experimental CO depletion rate was about equal to the transport rate in the case of V_L/V_G = 0.92.

Keywords: *Clostridium carboxidivorans*; syngas; ethanol; butanol; growth kinetics

1. Introduction

The continuous increase in the demand for energy and materials throughout the world—as a consequence of the rapid increase of the world population and of the growing industrialization of the developing countries—increased environmental pollution and the pressure on fossil resources. Apart from environmental fallout, exploitation of fossil resources strongly affects the economic and social worldwide scenario—resource country independence, natural resource cost, etc. A potential solution to these issues is offered by the exploitation of renewable sources processed under sustainable conditions [1,2].

Ethanol and higher chain alcohols (e.g., butanol) are potential substitutes of fossil fuels as well as of chemical building blocks [3]. Alcohols can be produced by processing renewable resources via thermochemical or biotechnological routes. The first generation processes were based on renewable resources in competition with food resources (e.g., starch, sugar, vegetable oils). Although production

of first generation biofuels in United States and in Brazil continues as a commercially mature technology, increasing criticism regarding ethical sustainability issues, addressed the European Community to promote attention towards second-generation biofuels [4].

Second-generation biofuels are produced by processing resources not in competition with food (e.g., lignocellulosic biomass). The bio-chemical route includes the conversion of cellulose and hemicellulose fraction of biomass feedstock to a mixture of fermentable reducing sugars, using enzymes or acid hydrolysis. The hydrolytic route is not sustainable—from an economic, energetic, and environmental point of view—when the lignin fraction is too high, even though the overall Carbon-fraction of the biomass is promising [5]. The thermochemical route might include the gasification/pyrolysis technology under high temperatures, to convert the lignocellulosic structure of biomass to intermediate gas (syngas) or liquid products. As a consequence, the thermochemical route is able to exploit all Carbon-fraction of the biomass. The gasification produces syngas—a mixture of carbon monoxide (CO), hydrogen (H₂), carbon dioxide (CO₂), methane (CH₄), and trace gases—that can be further processed.

The millions of tons of waste, e.g., stalk, food waste, waste gas etc., produced by anthropic activities, are a potential feedstock to produce bioenergy, along with solving environmental problems. Some industrial processes (e.g., oil refining, steelmaking, production of carbon black, methanol and coke, gasification, and pyrolysis) release a huge amount of waste gases, where CO and H₂ (syngas) are the main components. These waste gases can be used as raw materials for biological conversion into biofuel/biochemical, through fermentation. The syngas fermentation exploits microorganisms, such as acetogens, that are able to use a mixture of H₂, CO, and CO₂, to produce fuels and chemicals, such as ethanol, butanol, hexanol, acetic acid, butyric acid, and methane. *Clostridium carboxidivorans* is one of such microorganisms that is able to grow on synthesis gas, to produce liquid biofuels (ethanol and butanol) using a variation of the classical Wood–Ljungdahl pathway [6]. The industrial utilization of syngas can accelerate the recovery of carbon resources and decrease the dependence on fossil fuels. Syngas fermentation processes might also meet the strategic needs of the low-carbon development path. Therefore, studies on syngas fermentation are particularly necessary [7] to achieve industrial development of this process.

Fermentation process should overcome some issues. One of the challenges is related to the low water solubility of CO and other compounds (e.g., H₂), which limits the mass transport rate of the substrate to the liquid phase in suspended-growth bioreactors or to the biofilm in attached-growth bioreactors, limiting the production yield of (bio)fuels or platform chemicals of interest, at the same time. Some previous and on-going studies focus on minimizing such drawback. Among others, the use of membrane systems, as well as attached-growth bioreactors, seem to allow a more efficient mass transfer of poorly soluble compounds [8]; the use of micro-bubble spargers in suspended-growth bioreactors has the same effect [9]. Another drawback to be taken into account, and already previously observed in conventional acetone–butanol–ethanol (ABE) fermentation from carbohydrates, is solvent toxicity [10]. This is an important factor to take into account in butanol fermentation, as acetogenic bacterial cells rarely tolerate more than 2% butanol [11].

This study reports recent results regarding the conversion of CO into acids/alcohols, carried out by *Clostridium carboxidivorans*, a Gram positive, mesophilic, and obligate anaerobic carboxydrotroph. *C. carboxidivorans* is known to grow autotrophically with syngas and chemoorganotrophically with a great variety of sugars. It is able to ferment these carbon sources to produce acids and alcohols [12–14]. The bacterium was grown under batch conditions, with no pH control, and by using CO as the sole carbon source. The objective was to develop and optimize culture conditions to increase the production of acid/alcohols through anaerobic CO fermentation. In particular, this study aimed to assess the effects of the CO partial pressure on the microorganism growth kinetics and on fermentation performances.

2. Materials and Methods

2.1. Microorganism and Culture Media

Clostridium carboxidivorans DSM 15,243 was supplied by Deutsche Sammlung von Mikroorganismen und Zellkulturen (DSMZ) in the form of dried pellets. Stock cultures were reactivated according to the DSMZ procedure. A synthetic rich medium (Wilkins Chalgren Anaerobic Broth Base, WCAB) was used to rehydrate and reactivate the microorganism, and glycerol was used as the cryo-protective agent. Reactivated cultures were stored at $-80\text{ }^{\circ}\text{C}$. The thawed cells were inoculated into 12 mL of WCAB in 15 mL Hungate tubes (pre-cultures). Cells were grown under anaerobic conditions for 24 h at $35\text{ }^{\circ}\text{C}$, they were then transferred into fermentation bottles. Tests were carried out in triplicates (biological replicates) to support reproducibility. The reported results are the mean values.

The composition of the standard fermentation medium was [3]—1 g/L yeast extract; 25 mL/L mineral solution (a source of sodium, ammonium, potassium, phosphate, magnesium, sulfate, and calcium); 10 mL/L trace metal solution; 10 mL/L vitamin solution; 1 mL/L resazurin; and 0.60 g/L cysteine-HCl.

The mineral stock solution contained (per liter distilled water) 80 g NaCl, 100 g NH_4Cl , 10 g KCl, 10 g KH_2PO_4 , 20 g MgSO_4 , and 4 g CaCl_2 . The vitamin stock solution contained (per liter distilled water) 10 mg pyridoxine, 5 mg each of thiamine, riboflavin, calcium pantothenate, thioctic acid, para-amino benzoic acid, nicotinic acid, and vitamin B12, and 2 mg each of D-biotin, folic acid, and 2-mercaptoethane-sulfonic acid. The trace metal stock solution contained (per liter distilled water) 2 g nitrilotriacetic acid, 1 g manganese sulfate, 0.80 g ferrous ammonium sulfate, 0.20 g cobalt chloride, 0.20 g zinc sulfate, and 20 mg each of cupric chloride, nickel chloride, sodium molybdate, sodium selenate, and sodium tungstate [3].

All chemicals were from Sigma Aldrich (Milan, Italy).

2.2. Batch Tests

Fermentation tests were carried out in 250 mL serum bottles (DWK Life Sciences-Wheaton, Millville, NJ, USA). A pre-set volume of medium was loaded in bottles and boiled. The N_2 stream was sparged into the bottles during the cooling down of the medium. As the temperature of the medium reached $40\text{ }^{\circ}\text{C}$, 0.06 g/L cysteine-HCl was supplemented as the reducing agent, the pH was adjusted to 5.75 with 2 M NaOH, and N_2 was continuously flushed. The bottles were sealed with Viton stoppers, capped with aluminum crimps, and autoclaved for 20 min at $121\text{ }^{\circ}\text{C}$. The bottles were maintained under anaerobic conditions, they were pressurized with 100% CO and inoculated. Bottles were kept under agitation at 130 rpm on an orbital shaker, housed in an incubation chamber at $35\text{ }^{\circ}\text{C}$.

The initial culture medium was set at 55 mL and 120 mL. Therefore, the liquid-to-gas volume ratio (V_L/V_G) was 0.28 and 0.92, respectively. The CO pressure in the headspace was set between 0.5 and 2.5 atm. Tests carried out at 0.5 and 1.0 atm CO partial pressure were performed in mixture with N_2 (Total pressure = 1.5 and 2.0 atm, respectively). In all other tests, the reported initial CO pressures were the total pressures.

2.3. Analytical Methods

PH was measured off-line in 1.5 mL samples by a pH-meter (Hanna Instruments, Woonsocket, RI, USA).

One milliliter of culture was daily sampled from fermentation bottles. Each culture was characterized in terms of cell concentration and soluble products. The samples were centrifuged (13,000 rpm, 10 min) by using a centrifuge (Centrifuge MiniSpin[®], Eppendorf Italia, Milan, Italy), before analyzing the concentration of water-soluble products by HPLC (HP1100, Agilent Co., Santa Clara, CA, USA).

The optical density (OD_{λ}) was measured at 600 nm by using a UV-visible spectrophotometer (SPECORD 50 UV-VIS, Analytik Jena, Jena, Germany). The biomass concentration (g_{DM}/L) was

assessed by processing the measured absorbance, according to a previously generated calibration curve ($1 \text{ OD} = 0.4 \text{ g}_{\text{DM}}/\text{L}$).

The concentrations of water-soluble products—acetic acid, butyric acid, hexanoic acid, ethanol, and butanol—were measured by using an HPLC (HP1100, Agilent Co., Santa Clara, CA, USA), equipped with Rezex™ ROA-Organic Acid H⁺ column (8%), $150 \times 7.8 \text{ mm}$, and a UV detector at a wavelength of 284 nm, at room temperature. The mobile phase was 7 mM H₂SO₄ solution fed at 0.8 mL/min flow rate.

Gas samples of 3 mL were periodically taken from batch bottles to monitor the CO and CO₂ concentrations. Gas-phase CO/CO₂ concentrations were measured using a gas chromatograph (GC, HP6890, Agilent Co., Santa Clara, CA, USA) equipped with a thermal conductivity detector (TCD). The GC was fitted with a 15-mHP-PLOT Molecular Sieve 5A column (Internal Diameter, 0.53 mm; film thickness, 50 μm) (Sigma Aldrich, Milan, Italy). The pressure in the fermentation bottles was measured using a pressure manometer (Keller), before and after each gas sampling.

Liquid and gas measurements were processed to assess the parameters reported hereinafter:

- CO conversion (ξ_{CO}), the ratio between the CO converted and the CO fed at the beginning of the test;
- CO-to-product “i” yield coefficient ($Y_{i/\text{CO}}$), the ratio between the produced mass of product “i” (cells or acid/solvent), and the decrease of the CO mass during the same time interval;
- The specific cell growth rate (μ). It was estimated at the beginning of the exponential phase as the slope of the biomass concentration (X) vs. time curve, on a log scale.

3. Results and Discussion

3.1. CO Fermentation

The aim of this work was to assess the effects of the CO partial pressure in the headspace of the fermenter on the microorganism growth kinetics and on the fermentation performances. Tests to characterize cell growth and acids/solvents production under different CO pressure were carried out using batch fermenters. The CO pressure in the headspace was set between 0.5 and 2.5 atm. Tables 1 and 2 report relevant data of fermentation tests carried out by setting the liquid/gas volumetric ratio at 0.28 and 0.92, respectively. Results were reported in terms of—maximum concentration of cells (X), ethanol (E), butanol (B), acetic acid (AA), butyric acid (BA), and hexanoic acid (HA). CO to ethanol yield ($Y_{\text{E}/\text{CO}}$), CO conversion degree (ξ_{CO}), and specific cell growth rate (μ) are also reported. No data were reported on hexanol because the corresponding production rate was negligible. Each test was carried out in triplicates (biological replicates). Data reported in tables and figures are the mean values between them. The standard error was always lower than 2%.

Table 1. Data from the fermentation tests carried out by setting the liquid volume at 55 mL ($V_L/V_G = 0.28$). X, cell concentration; AA, acetic acid concentration; BA, butyric acid concentration; HA, hexanoic acid concentration; E, ethanol concentration; B, butanol concentration; $Y_{E/CO}$, CO-to-ethanol yield coefficient; ξ_{CO} , CO conversion degree; μ , specific cell growth rate.

P_{CO} atm	X g _{DM} /L	AA mg/L	BA mg/L	HA mg/L	E mg/L	B mg/L	$Y_{E/CO}$ g/g	ξ_{CO} %	μ h ⁻¹
0.5	$0.67 \pm 1.2 \times 10^{-2}$	1280 ± 20	325 ± 6	145 ± 2	130 ± 2	70 ± 1	$0.063 \pm 1.2 \times 10^{-3}$	97.9 ± 0.7	$0.088 \pm 1.5 \times 10^{-3}$
1.0	$0.61 \pm 1.1 \times 10^{-2}$	1740 ± 25	320 ± 4	140 ± 1	220 ± 4	110 ± 2	$0.049 \pm 9 \times 10^{-4}$	94.2 ± 0.5	$0.100 \pm 5.5 \times 10^{-4}$
1.5	$0.68 \pm 1.3 \times 10^{-2}$	1550 ± 15	345 ± 5	250 ± 4	315 ± 5	120 ± 2	$0.097 \pm 1.7 \times 10^{-3}$	49.5 ± 0.8	$0.094 \pm 7.2 \times 10^{-4}$
1.7	$0.68 \pm 1.4 \times 10^{-2}$	1620 ± 30	380 ± 4	210 ± 1	400 ± 7	130 ± 1	$0.094 \pm 1.5 \times 10^{-3}$	57.0 ± 0.6	$0.092 \pm 1.8 \times 10^{-3}$
2.0	$0.68 \pm 1.2 \times 10^{-2}$	1200 ± 23	390 ± 5	285 ± 3	380 ± 6	100 ± 2	$0.11 \pm 2 \times 10^{-3}$	39.0 ± 0.7	$0.099 \pm 1.2 \times 10^{-3}$
2.2	$0.73 \pm 1.4 \times 10^{-2}$	1600 ± 20	405 ± 6	230 ± 4	230 ± 4	105 ± 2	$0.061 \pm 1.1 \times 10^{-3}$	44.1 ± 0.8	$0.086 \pm 4.2 \times 10^{-3}$
2.3	$0.53 \pm 1 \times 10^{-2}$	970 ± 12	390 ± 6	250 ± 3	180 ± 3	110 ± 2	$0.047 \pm 9 \times 10^{-4}$	29.3 ± 0.5	$0.086 \pm 1.5 \times 10^{-3}$
2.5	$0.62 \pm 1.1 \times 10^{-2}$	950 ± 10	380 ± 4	290 ± 2	150 ± 2	105 ± 1	$0.043 \pm 8 \times 10^{-4}$	31.7 ± 0.6	$0.089 \pm 9 \times 10^{-4}$

Table 2. Data from the fermentation tests carried out by setting the liquid volume at 120 mL ($V_L/V_G = 0.92$).

P_{CO} atm	X g _{DM} /L	AA mg/L	BA mg/L	HA mg/L	E mg/L	B mg/L	$Y_{E/CO}$ g/g	ξ_{CO} %	μ h ⁻¹
0.5	$0.38 \pm 7 \times 10^{-3}$	715 ± 10	85 ± 1	70 ± 1	120 ± 2	25 ± 0.5	$0.17 \pm 3 \times 10^{-3}$	100 ± 0	$0.072 \pm 3 \times 10^{-4}$
1.0	$0.34 \pm 6 \times 10^{-3}$	800 ± 15	100 ± 2	60 ± 1.1	115 ± 2	25 ± 0.4	$0.076 \pm 1.5 \times 10^{-3}$	99.9 ± 0.1	$0.081 \pm 2 \times 10^{-4}$
1.5	$0.40 \pm 7 \times 10^{-3}$	800 ± 10	110 ± 2	80 ± 1.5	120 ± 2	35 ± 0.3	$0.059 \pm 1.1 \times 10^{-3}$	98.4 ± 0.5	$0.075 \pm 3 \times 10^{-3}$
1.7	$0.35 \pm 7 \times 10^{-3}$	1110 ± 20	124 ± 2	80 ± 1.4	130 ± 2	45 ± 0.7	$0.056 \pm 1.1 \times 10^{-3}$	97.2 ± 0.4	$0.072 \pm 1.3 \times 10^{-3}$
2.0	$0.42 \pm 8 \times 10^{-3}$	1580 ± 25	176 ± 3	85 ± 1.2	225 ± 3	70 ± 0.5	$0.067 \pm 1.3 \times 10^{-3}$	94.2 ± 0.5	$0.086 \pm 8 \times 10^{-4}$
2.2	$0.47 \pm 8 \times 10^{-3}$	1870 ± 25	230 ± 4	90 ± 1.4	190 ± 2	75 ± 1	$0.062 \pm 1.2 \times 10^{-3}$	100 ± 0	$0.062 \pm 7 \times 10^{-4}$
2.3	$0.39 \pm 7 \times 10^{-3}$	1500 ± 20	130 ± 2	80 ± 1.3	90 ± 2	60 ± 1.2	$0.031 \pm 6 \times 10^{-4}$	92.6 ± 0.7	$0.065 \pm 5 \times 10^{-4}$
2.5	$0.38 \pm 7 \times 10^{-3}$	1520 ± 10	100 ± 1	60 ± 1	90 ± 1	80 ± 1.1	$0.030 \pm 6 \times 10^{-4}$	86.8 ± 0.8	$0.060 \pm 1.1 \times 10^{-3}$

Figure 1 reports time resolved data of pH, cell (X), and metabolite (B, E, AA, BA, HA) concentration, measured during batch fermentation tests carried out in batch bottles, setting the liquid/gas volume ratio at 0.28 and the initial CO pressure at 1.7 atm. *C. carboxidivorans* started to grow since the inoculation, and the lag phase was negligible. Maximum biomass concentration (0.68 $\text{g}_{\text{DM}}/\text{L}$) was at about 46 h (Figure 1A), and maximum concentration of AA, BA, and HA (about 1600, 370, and 205 mg/L , respectively) were measured later, at about 60 h (Figure 1B). Acids were detected since 24 h and increased continuously with time, approaching a constant value after about 70 h. The initial pH of the medium was set at 5.6 in this test. During the acetogenic phase, medium acidification was observed because no pH control was used during the fermentation tests. The pH decreased gradually with time and approached the minimum of about 4.6, at the end of the test. Ethanol and butanol concentration departed from zero after about 24 h, and increased with time up to about 395 and 130 mg/L , respectively, after about 70 h (Figure 1B). Solvent production was not coupled with acid consumption—solvent concentration (ethanol and butanol) increased with time without any reduction of acid concentration. The observed path to produce solvents was not in agreement with previous results reported by Abubackar et al. [15] for CO fermentation by *C. autoethanogenum* and the expected path for clostridia known for the ABE fermentation from carbohydrates. In particular, Abubackar et al. [15] pointed out that CO was converted into acetic acid and ethanol was produced by conversion of the accumulated acetic acid. Therefore, two possible scenarios might be inferred—(i) alcohols were formed directly from the conversion of CO ; and (ii) alcohols were produced by acid conversion and the acid production balanced any acid consumption.

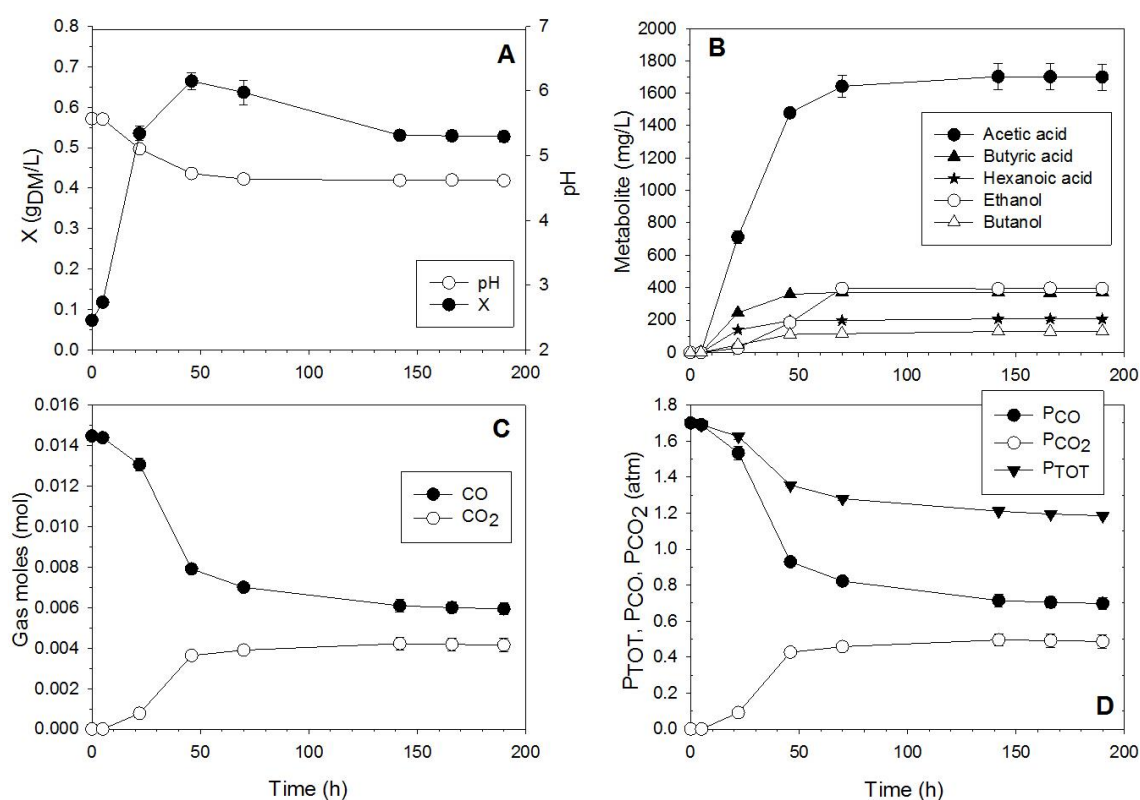


Figure 1. Data vs. time measured during a batch fermentation—initial $P_{\text{CO}} = 1.7$ atm; $V_{\text{L}}/V_{\text{G}} = 0.28$. (A) Cell concentration and pH; (B) metabolite concentration; (C) CO/CO_2 moles temporal profiles in the headspace of bottles; and (D) total and partial CO/CO_2 pressure in the headspace of bottles.

CO consumption was assessed during the fermentation test. Figure 1C reports the moles of CO and CO_2 in the bottles headspace; Figure 1D reports total pressure and partial pressure of CO and CO_2 measured in the headspace. The analysis of Figure 1 points out that bacterial growth and metabolites

production were coupled with CO consumption and CO₂ production. After 200 h, about 57% of the initial CO was consumed. From the analysis of Figure 1C,D, it was also evident that the rate of CO consumption increased as the cell concentration increased at the beginning of the fermentation, to slow down as acid concentration increased.

3.2. Effect of the CO Pressure

The effect of CO partial pressure on growth kinetics and metabolite production was assessed by setting the initial P_{CO} between 0.5 and 2.5 atm (Tables 1 and 2) (tests at 0.5 and 1.0 atm CO pressure were carried out in mixture with N₂, total pressure = 1.5 and 2.0 atm; in all other tests, the reported initial pressures were total pressures). From the analysis of data reported in Tables 1 and 2, the results showed that:

- P_{CO} affected maximum cell concentration measured during fermentation tests. Maximum cell concentration was about 0.7 g_{DM}/L for initial P_{CO} between 0.5 and 2.2 atm, and decreased at higher initial P_{CO} . Substrate inhibition might be responsible for the decrease of cell growth with P_{CO} .
- CO conversion measured during fermentation tests carried out at $V_L/V_G = 0.28$, decreased with initial P_{CO} . CO conversion was almost total at low initial P_{CO} (0.5 and 1 atm), and it significantly decreased as initial P_{CO} was higher than 1 atm.
- The best performance in terms of ethanol/butanol production was obtained with $V_L/V_G = 0.28$ at initial $P_{CO} = 1.7$ atm.

Figure 2 reports the measured specific cell growth rate (μ) as a function of CO concentration in the liquid phase. It was assumed that at the beginning of the fermentation, CO concentration in the liquid phase (CO*) was under equilibrium conditions with the gas phase. Specific growth rate was calculated for each initial CO concentration by plotting $\ln(X)$ vs. time. The experimental data would suggest that—(i) specific cell growth rate was affected by the CO concentration, according to the substrate inhibition behavior; (ii) specific cell growth rate was affected by the amount of CO available for unit of liquid volume.

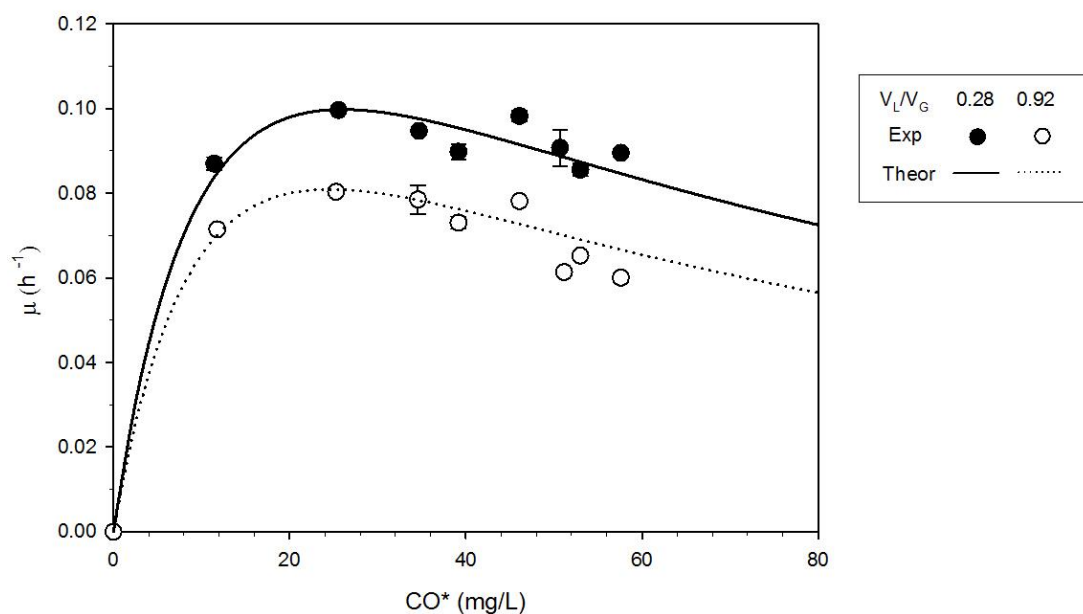


Figure 2. Specific cell growth rate of *C. carboxivorans* as a function of initial CO concentration in the liquid phase—it was assumed that at the beginning of the fermentation the CO in the liquid phase (CO*) was under equilibrium conditions with the gas phase. Lines are the plot of Equation (1) (parameters in Table 3).

Table 3. Kinetic parameters assessed by the regression of experimental data, according to the proposed model (Equation (1)).

V_L/V_G	$\mu_{\max} \text{ h}^{-1}$	$K_M \text{ mg/L}$	$K_I \text{ mg/L}$
0.28	0.22	15	45
0.92	0.18	15	40

Kinetic data were processed according to an unsegregated–unstructured model—the Haldane model (Equation (1)) characterized by substrate inhibition was used (μ_{\max} , K_M and K_I parameters of the model).

$$\mu = \mu_{\max} \left(\frac{CO^*}{CO^* + K_M + \frac{CO^{*2}}{K_I}} \right) \quad (1)$$

Data regression according to Equation (1) provided the kinetic parameters reported in Table 3.

The plot of the expected values of μ , assessed according to Equation (1), is reported in Figure 2. The good agreement between experimental data and expected values ($R^2 = 0.88$) supported that *C. carboxidivorans* growth rate was characterized by CO inhibition within the investigated range of CO concentration. In particular, the optimal P_{CO} was 1.1 atm (corresponding to a dissolved CO concentration of about 25 mg/L), for both the V_L/V_G used.

Substrate inhibition occurred during the initial oxidation of the electron donor substrates, and reduced or stopped the oxidation of the electron donor, through either competitive or non-competitive inhibition, resulting in slow substrate consumption rates [16]. In particular, CO was a substrate that showed a substrate inhibitory effect above a critical concentration because CO inhibits metalloenzymes by forming stable complexes, resulting in reduced enzyme activity. Notably, most enzymes in the acetyl-CoA pathway possess redox activities due to their metallic centers [17]. Yasin et al. [18] reported the observed behavior of the specific growth rate vs. CO concentration (CO inhibition) for different microorganisms. High pressure fermentation could be detrimental when the dissolved CO concentration was greater than the kinetic requirements of the microbes; therefore, identifying the optimum dissolved CO concentration was necessary to design and control large-scale fermenters.

Hurst and Lewis [19] assessed the effects of constant CO partial pressure, ranging from 0.35 to 2.0 atm, on cell growth, acetic acid production, and ethanol production, using *Clostridium carboxidivorans*. They did not experience substrate inhibition on cell growth rate. A possible explanation of this different behavior with respect to the one reported in this work could be related to the different gas composition used. Indeed, Hurst and Lewis [19] used a mixture of CO and CO₂. Therefore, it was not possible to distinguish between the effect of CO and CO₂ (double substrate) on the growth rate.

Moreover, Fernandez et al. [6] pointed out that product inhibition had a significant effect on cell growth and acid/solvent production. However, the inhibitory effect of the acids and solvents was not taken into account in this study because the specific growth rate was estimated at the beginning of the exponential phase—the metabolite concentrations were more than 10-fold lower than the inhibitory concentrations reported in the literature [20].

Other studies reported in the literature used CO as the sole carbon/electron source. Nevertheless, to the authors' knowledge, models/kinetics to describe *C. Carboxidivorans* fermentation are still scarce in the literature, and only a few authors have attempted to adjust kinetic expressions to experimental data, even though, identifying the microorganism growth kinetics (and thus, the optimum dissolved CO concentration) is necessary to design and control large-scale fermenters. Younesi et al. [21] and Mohammadi et al. [22] adjusted the logistic curves to the growth of *Clostridium ljungdahlii* on artificial syngas, using experimental data from batch fermentation essays in serum bottles. Mohammadi et al. [22] were also able to fit Gompertz equations to their experimental profiles of product formation, and uptake rate equations for CO, presenting estimations of kinetic parameters.

A possible strategy to obtain kinetics information on *C. Carboxidivorans* would be to fit the model parameters with literature data. However, this procedure turned out to be a challenge due to several reasons. First, the number of experimental papers on syngas fermentation is relatively small, compared to other types of fermentation; moreover, an even smaller number provides data with coproduction of higher alcohols such as butanol. Among these, some provide exploratory data of very long cultures in which several accidents or interventions occur, and others fail to provide clear information about the process conditions (e.g., often the gas flow rates are omitted from the text, probably because they were not fixed during the experiment). Therefore, the authors thought that a systematic study dealing with both data acquisition and their elaboration for kinetics assessment was necessary before moving to other topics, such as bioreactor design.

3.3. Effect of the Gas-to-Liquid Volume Ratio

Tests carried out under different liquid-to-gas volume ratio (V_L/V_G) pointed out that cell growth was affected by this operating condition. Cultures carried out at $V_L/V_G = 0.28$ were characterized by a growth rate higher than that measured for cultures carried out at $V_L/V_G = 0.92$ (Tables 1 and 2).

Time resolved data of CO in the gas phase of bottles are reported in Figure 3, for the cultures carried out at $V_L/V_G = 0.28$ and $V_L/V_G = 0.92$ and initial $P_{CO} = 2$ atm. As expected, CO in the bottle headspace decreased with time. Tests carried out at $V_L/V_G = 0.92$ were characterized by higher CO uptake rates with respect to tests carried out at $V_L/V_G = 0.28$. Moreover, CO depletion was recorded for the tests carried out at $V_L/V_G = 0.92$.

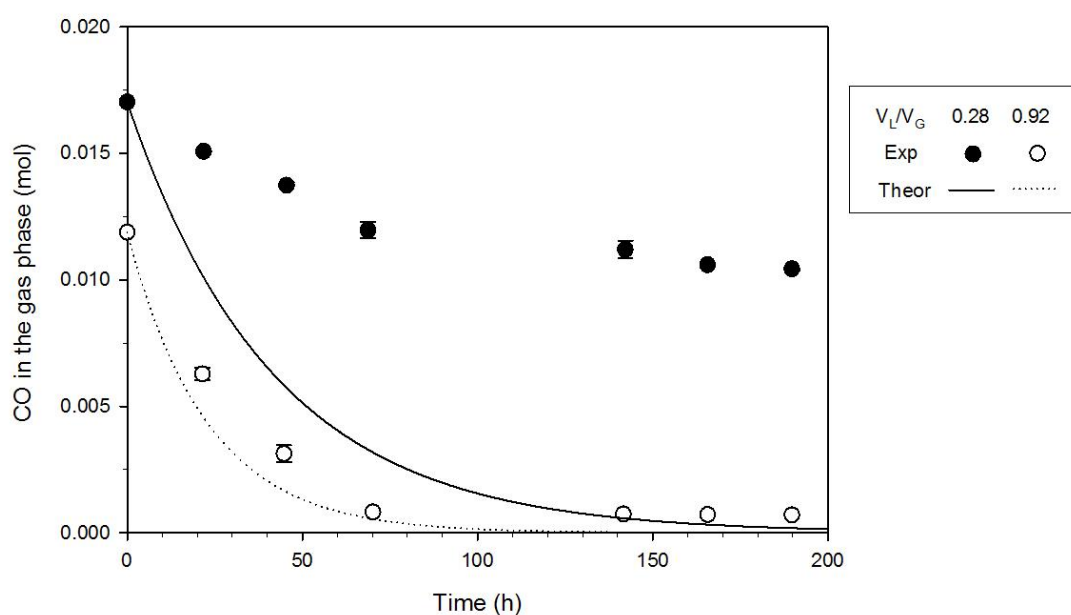


Figure 3. CO in the headspace vs. fermentation time. Initial $P_{CO} = 2$ atm. Experimental data and plots of Equation (4).

The increase of μ as V_L/V_G decreased was interpreted by taking into account the mass of CO available for cells and the gas-to-liquid transport rate. In particular, the competition between CO uptake and CO transport between the gas and liquid phases was addressed.

Data of CO moles and cell density (Tables 1 and 2) measured during tests carried out at the same initial P_{CO} were processed to assess the amount of CO available for the unit of cell mass, as a function of fermentation time. Figure 4 reports the moles of CO per gram of bacterial mass for the tests carried out at $P_{CO} = 2$ atm. As expected, the CO per gram of bacterial mass was larger for the $V_L/V_G = 0.28$ cultures, throughout the fermentation tests. For both V_L/V_G used, the CO per gram of bacteria decreased with

time and approached a constant value. In particular, CO depletion was recorded for the test carried out at $V_L/V_G = 0.92$, as the fermentation time was larger than 74 h.

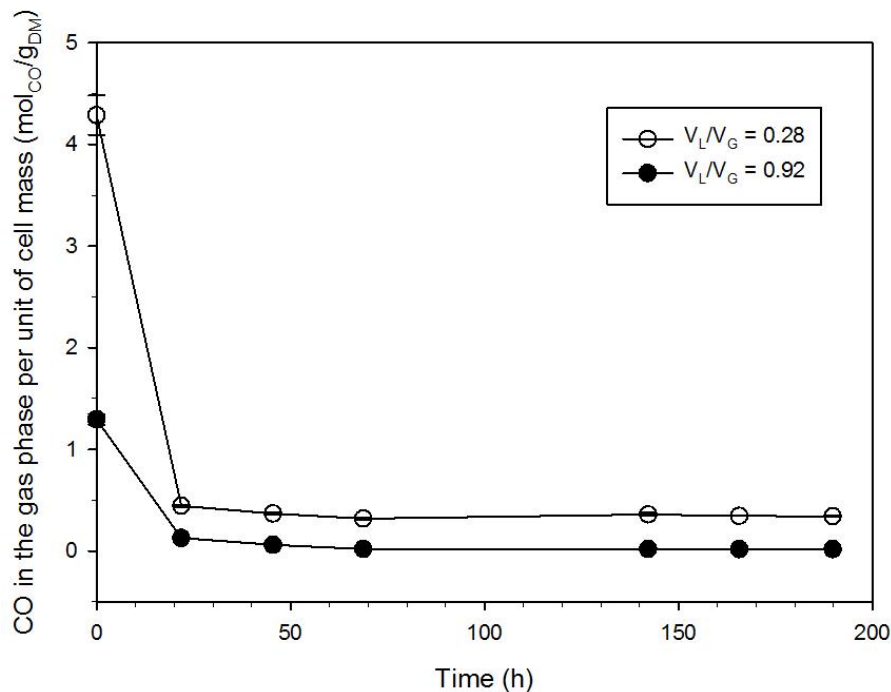


Figure 4. CO in the bottle headspace per unit of cell mass. Initial $P_{CO} = 2$ atm.

CO transport rate from the gas-to-liquid phase was assessed to verify if the specific cell growth rate was controlled by mass transport phenomena. According to Frankman [23], the volumetric mass transport coefficient ($k_L a$) for CO was 4.69 h^{-1} and 2.64 h^{-1} for the bottles operated at $V_L/V_G = 0.28$ and 0.92 , respectively. The mass balance referred to CO and extended to the bottle headspace yields:

$$\frac{dn_{CO}}{dt} = -k_{LaCO}(CO^* - CO) \quad (2)$$

where n_{CO} is the CO mole number, CO is the concentration of CO in the liquid phase, k_{LaCO} is the mass transport coefficient for CO referred to the liquid volume, CO^* is the liquid concentration under equilibrium conditions with the gas phase. Under conditions characterized by very fast CO conversion in liquid phase, the process overall rate was mass-transport controlled. The CO mass-transport rate was maximum because CO in the liquid phase was 0, CO was promptly converted as it flowed into the culture, and Equation (2) yielded:

$$\frac{dn_{CO}}{dt} = -k_{LaCO}CO^* = -k_{LaCO}\frac{P_{CO}}{H_{CO}} = -k_{LaCO}\frac{\left(\frac{n_{CO}RT}{V_G}\right)}{H_{CO}} \quad (3)$$

where H_{CO} is the Henry constant referred to CO, T is the temperature, and R is the universal gas constant. Integration of Equation (3), with respect to time yields:

$$n_{CO} = n_{CO}^0 \exp\left(\frac{-k_{LaCO}\left(\frac{RT}{V_G}\right)}{H_{CO}}\right)t \quad (4)$$

Under mass-transport control conditions, CO in bottle headspace changed with time, according to Equation (4). Figure 3 reports the plot of Equation (4) for both values of V_L/V_G . The comparison between experimental data and expected CO depletion in the headspace pointed out that the mass

transport phenomena did not control CO uptake for $V_L/V_G = 0.28$ —transport phenomena were able to pump CO into the culture at sufficient rate. On the contrary, expected CO depletion in the headspace for tests carried out at $V_L/V_G = 0.92$, was close to that measured—the experimental CO depletion rate was about the transport rate. These results were in accordance with the ones reported by Frankman (2009) [23].

As a consequence of the reported analysis on the effects of the V_L/V_G ratio, the characterization of kinetics and fermentation stoichiometry carried out at $V_L/V_G = 0.28$ was more reliable than those carried out at $V_L/V_G = 0.92$.

4. Conclusions

The present study aimed at assessing the effects of CO pressure on growth kinetics and on fermentation performances of *C. carboxidivorans*. The results showed that:

- P_{CO} affected microorganism growth kinetics; indeed, *C. carboxidivorans* growth rate was characterized by CO inhibition within the investigated range of CO concentration, and the optimal P_{CO} was 1.1 atm (corresponding to a dissolved CO concentration of about 25 mg/L) for both the V_L/V_G used.
- Growth differences were observed when the gas-to-liquid volume ratio was changed; the mass-transport phenomena did not control CO uptake for $V_L/V_G = 0.28$; on the contrary, the experimental CO depletion rate was about equal to the transport rate in the case of $V_L/V_G = 0.92$. Therefore, the characterization of kinetics and fermentation stoichiometry carried out at $V_L/V_G = 0.28$ was more reliable than those carried out at $V_L/V_G = 0.92$.

Author Contributions: Conceptualization, F.R., A.M. and M.E.R.; methodology, F.L., G.R. and F.R.; software, F.L., G.R. and F.R.; validation, F.L., G.R. and F.R.; formal analysis, F.L. and G.R.; investigation, F.L., G.R. and F.R.; resources, F.L., G.R. and F.R.; data curation, F.L., G.R. and F.R.; writing—original draft preparation, F.L.; writing—review and editing, F.R. and A.M.; visualization, F.L., G.R. and F.R.; supervision, F.R., A.M. and M.E.R.; project administration, A.M.; funding acquisition, A.M. All authors have read and agreed to the published version of the manuscript.

Funding: This research was funded by Ministero dell’Istruzione, dell’Università e della Ricerca, grant number ARS01_00985.

Conflicts of Interest: The authors declare no conflict of interest.

Nomenclature

AA	Acetic acid concentration (mg/L)
B	butanol concentration (mg/L);
BA	Butyric acid concentration (mg/L);
CO	concentration of CO in the liquid phase (mg/L);
CO *	liquid concentration of CO under equilibrium conditions with the gas phase (mg/L)
E	Ethanol concentration (mg/L)
HA	Hexanoic acid concentration (mg/L)
H_{CO}	Henry constant referred to CO (atm *L/mol)
k_{LaCO}	volumetric mass transport coefficient for CO (h^{-1})
K_M, K_I	parameters of the Haldane model (mg/L)
n_{CO}	CO mole number (mol)
P_{CO}	CO partial pressure (atm)
R	universal gas constant (L *atm/K/mol)
T	Fermentation temperature (K)
V_G	Gas volume in serum bottles (mL)
V_L	Liquid volume in serum bottles (mL);
X	cell concentration (g_{DM}/L);
$Y_{i/CO}$	CO-to-product “i” yield coefficient (g/g);
μ	specific cell growth rate (h^{-1})

μ_{\max}	maximum specific cell growth rate (h^{-1})
ξ_{CO}	CO conversion degree (-)

References

- Gowen, C.M.; Fong, S.S. Applications of systems biology towards microbial fuel production. *Trends Microbiol.* **2011**, *10*, 516–524. [[CrossRef](#)] [[PubMed](#)]
- Abdehagh, N.; Tezel, F.H.; Thibault, J. Separation techniques in butanol production: Challenges and developments. *Biomass Bioenergy* **2014**, *60*, 222–246. [[CrossRef](#)]
- Fernández-Naveira, Á.; Abubackar, H.N.; Veiga, M.C.; Kennes, C. Efficient butanol-ethanol (B-E) production from carbon monoxide fermentation by *Clostridium carboxidivorans*. *Appl. Microbiol. Biotechnol.* **2016**, *100*, 3361–3370. [[CrossRef](#)] [[PubMed](#)]
- Mohammadi, M.; Najafpour, G.D.; Younesi, H.; Lahijani, P.; Uzir, M.H.; Mohamed, A.R. Bioconversion of synthesis gas to second generation biofuels: A review. *Renew. Sustain. Energy Rev.* **2011**, *15*, 4255–4257. [[CrossRef](#)]
- Fernandez-Naveira, A.; Veiga, M.C.; Kennes, C. Production of higher alcohols through anaerobic H–B–E fermentation of syngas or waste gas. *Chem. Technol. Biotechnol.* **2017**, *92*, 712–713. [[CrossRef](#)]
- Fernandez-Naveira, A.; Abubackar, H.N.; Veiga, M.C.; Kennes, C. Production of chemicals from C1 gases (CO, CO₂) by *Clostridium carboxidivorans*. *World J. Microbiol. Biotechnol.* **2017**, *33*, 43. [[CrossRef](#)]
- Stoll, K.I.; Herbig, S.; Sauer, J.; Neumann, A.; Oswald, F. Fermentation of H₂ and CO₂ with *Clostridium ljungdahlii* at elevated process pressure—first experimental results. *Chem. Eng. Trans.* **2018**, *64*, 2–7.
- Jin, Y.; Guo, L.; Veiga, M.C.; Kennes, C. Optimization of the treatment of carbon monoxide-polluted air in biofilters. *Chemosphere* **2009**, *74*, 332–337. [[CrossRef](#)]
- Bredwell, M.D.; Worden, R.M. Mass-transfer properties of microbubbles. 1. Experimental studies. *Biotechnol Prog* **1998**, *14*, 31–38. [[CrossRef](#)]
- Raganati, F.; Procentese, A.; Olivieri, G.; Russo, M.E.; Salatino, P.; Marzocchella, A. Biobutanol production from hexose and pentose sugars. *Chem. Eng. Trans.* **2014**, *38*, 193–198.
- Procentese, A.; Raganati, F.; Olivieri, G.; Russo, M.E.; Salatino, P.; Marzocchella, A. Continuous lactose fermentation by *Clostridium acetobutylicum*—Assessment of solventogenic kinetics. *Bioresour. Technol.* **2015**, *180*, 330–337. [[CrossRef](#)] [[PubMed](#)]
- Liou, J.S.C.; Balkwill, D.L.; Drake, G.R.; Tanner, R.S. *Clostridium carboxidivorans* sp. nov., a solvent-producing clostridium isolated from an agricultural settling lagoon, and reclassification of the acetogen *Clostridium scatologenes* strain SL1 as *Clostridium drakei* sp. nov. *Int. J. Syst. Evol. Microbiol.* **2005**, *55*, 2085–2091. [[CrossRef](#)] [[PubMed](#)]
- Liu, T.; Jiaqiang, E.; Yang, J.W.; Hui, A.; Cai, H. Development of a skeletal mechanism for biodiesel blend surrogates with varying fatty acid methyl esters proportion. *Appl. Energy* **2016**, *162*, 278–288. [[CrossRef](#)]
- Phillips, J.R.; Atiyeh, H.K.; Tanner, R.S.; Torres, J.R.; Saxena, J.; Wilkins, M.R.; Huhnke, R.L. Butanol and hexanol production in *Clostridium carboxidivorans* syngas fermentation: Medium development and culture techniques. *Bioresour. Technol.* **2015**, *190*, 114–121. [[CrossRef](#)] [[PubMed](#)]
- Abubackar, H.N.; Veiga, M.C.; Kennes, C. Carbon monoxide fermentation to ethanol by *Clostridium autoethanogenum* in a bioreactor with no accumulation of acetic acid. *Bioresour. Technol.* **2015**, *186*, 122–127. [[CrossRef](#)]
- Rittmann, B.E.; McCarty, P.L. *Environmental Technology: Principles and Applications*; McGraw-Hill: New York, NY, USA, 2005.
- Ragsdale, S.W. Life with carbon monoxide. *Crit. Rev. Biochem. Mol. Biol.* **2004**, *39*, 165–195. [[CrossRef](#)]
- Yasin, M.; Jeong, Y.; Park, S.; Jeong, J.; Lee, E.Y.; Lovitt, R.W.; Kim, B.H.; Lee, J.; Chang, I.S. Microbial synthesis gas utilization and ways to resolve kinetic and mass-transfer limitations. *Bioresour. Technol.* **2015**, *177*, 361–374. [[CrossRef](#)]
- Hurst, K.M.; Lewis, R.S. Carbon monoxide partial pressure effects on the metabolic process of syngas fermentation. *Biochem. Eng. J.* **2010**, *48*, 159–165. [[CrossRef](#)]

20. Fernandez-Naveira, A.; Abubackar, H.N.; Veiga, M.C.; Kennes, C. Carbon monoxide bioconversion to butanol-ethanol by *Clostridium carboxidivorans*: Kinetics and toxicity of alcohols. *Appl. Microbiol. Biotechnol.* **2016**, *100*, 4231–4240. [[CrossRef](#)]
21. Younesi, H.; Najafpour, G.; Mohamed, A.R. Ethanol and acetate production from synthesis gas via fermentation processes using anaerobic bacterium, *Clostridium ljungdahlii*. *Biochem. Eng. J.* **2005**, *27*, 110–119. [[CrossRef](#)]
22. Mohammadi, M.; Mohamed, A.R.; Najafpour, G.D.; Younesi, H.; Uzir, M.H. Kinetic studies on fermentative production of biofuel from synthesis gas using *Clostridium ljungdahlii*. *Sci. World J.* **2014**, *2014*, 910590. [[CrossRef](#)] [[PubMed](#)]
23. Frankman, A.W. Redox, Pressure and Mass Transfer Effects on Syngas Fermentation. Master's Thesis, Brigham Young University, Provo, UT, USA, 2009.



© 2020 by the authors. Licensee MDPI, Basel, Switzerland. This article is an open access article distributed under the terms and conditions of the Creative Commons Attribution (CC BY) license (<http://creativecommons.org/licenses/by/4.0/>).